Kinetic Reaction Analysis of an Anhydride-Cured Thermoplastic Epoxy: PGE/NMA/BDMA

Wei Chian† and Delmar C. Timm*

Department of Chemistry and Chemical Engineering, South Dakota School of Mines, Rapid City, South Dakota 57701, and Department of Chemical Engineering, University of Nebraska−Lincoln, Lincoln, Nebraska 68588

Received April 12, 2004; Revised Manuscript Received July 14, 2004

ABSTRACT: A comprehensive reaction analysis of a linear epoxy resin cured with an anhydride was performed to evaluate the reaction rate expressions. Monomers included phenyl glycidyl ether and methyl-5-norbornene-2,3-dicarboxylic anhydride or nadic methyl anhydride; the catalyst was *N*,*N*-dimethylbenzylamine; the initiator was *n*-propanol. Emphasis was initially placed on the molar dynamics of monomeric and oligomeric molecules. Molecular fractionations were achieved using reversed phase, high performance liquid chromatography. Chemical reaction rate constants were examined as a function of degree of polymerization. For the chain-initiated polymerization, the initiation rate constant was observed to be approximately 3 times greater than the propagation constant associated with oligomeric molecules. Both Poisson and Gold distributions were used to fit data. Examinations of polymeric fractions obtained by gel permeation chromatography in conjunction with a multiangle laser light scattering photometer revealed a minor side reaction that broadened the polydispersity index and resulted in the reduction of the cumulative, molar concentration of molecules as a function of conversion.

Introduction

Anhydride-cured epoxy resins often serve as the matrix for advanced, fiber-reinforced composites used in a variety of aerospace, structural, and sporting applications where high specific strength and stiffness, combined with good thermal stability, offer unique design advantages. To achieve optimal mechanical performance within the matrix, basic understanding between relationships that correlate molecular chain topology and physical properties is desired. At temperatures in excess of the glass transition temperature, the equilibrium modulus correlates with network structure through the theory of rubbery elasticity. Network structure in turn is dependent on the underlying chemical reactions and extent of cure. At temperatures below the glass transition temperature, shear bands and associated compressive stress/strain data reflect cross-link structure. To predict cross-linked chain topology, accurate chemical reaction models must be known. In this regard, phenyl glycidyl ether (PGE) serves as a model compound for diglycidyl ether of Bisphenol A (DGEBA) due to similar chemical structures. The former forms soluble resins comprised of linear chains; the latter forms a sol−gel network due to an increase in the chemical functionality of the monomer.

Using FTIR analyses, Antoon and Koenig[1] reported on chemical intermediates as a function of conversion in formulations based on DGEBA, methyl-5-norbornene-2,3-dicarboxylic anhydride or nadic methyl anhydride (NMA), and the catalyst *N*,*N*-dimethylbenzylamine (BDMA). Trappe et al.[2] relied on NMR analysis at high conversions and reported consistent observations for a thermoplastic formulated from PGE, phthalic anhydride, and 1-methylimidazole. Matějka et al.[3] and Luston et al.[4] also examined the associated chemical reactions. Kinetic reaction models have also incorporated observations associated with extents of reaction,[1,5,6,7] molecular dynamics observed through fractionations by gel permeation chromatography (GPC)[8] and heats of reaction observed with differential scanning calorimetry.[9−11] Reaction rate expressions reported differ from first- to third-order.

Nielsen et al.[8] and Tadros and Timm[6] studied the PGE/NMA/BDMA polymerization and condensed mechanistic models appearing in the literature into a propagation reaction. The reader that is interested in the anionic, chain-growth mechanism and chemical intermediates may consult these references and Antoon and Koenig.[1] In terms of reactive end groups, the tertiary amine catalyst associates with an alcohol, forming a hydrogen-bonded hydroxyl intermediate. The reaction was assumed to be at equilibrium. The hydrogen-bonded hydroxyl rapidly reacts with the anhydride, initially forming a tertiary amine/hydroxyl/anhydride transition state intermediate, which rapidly experiences rearrangement, forming an ester plus a hydrogen-bonded carboxylic acid/tertiary amine. This entity was assumed to be in equilibrium with a carboxyl/tertiary amine salt. The rate-limiting step inserts the oxirane into the hydrogen-bonded acid/catalyst group, yielding an ester plus re-forming a hydrogen-bonded hydroxyl complex. The reaction sequence causes the degree of polymerization to increment. By coupling equilibrium constraints, a stationary-state approximation for the hydrogen-bonded hydroxyl/tertiary amine complex with the rate-limiting reaction involving the hydrogen-bonded carboxyl acid/tertiary amine complex and an oxirane, Nielsen et al.[8] showed that the anionic, chain-growth polymerization reaction could be approximated by a greatly simplified propagation reaction between a molecule of degree of polymerization *j* and the oxirane monomer. The resultant overall kinetic reaction analysis predicted a Poisson population density distribution (PDD). Improvements in the fractionation capabilities of GPC and high performance liquid chromatography

* Corresponding author. University of Nebraska−Lincoln.
† South Dakota School of Mines.

10.1021/ma049293x CCC: $27.50
Published on Web 09/17/2004

warrant additional analysis.

The polymerization is controlled by a chain-initiated mechanism. Thus, the ratio of initiator to monomer formulated controls the ultimate molecular weight. In the current studies, low and high molecular weight PGE/NMA/BDMA resins were prepared using *n*-propanol as an initiator. Quantitative evaluation of PDDs were achieved using reversed-phase high performance liquid chromatography (HPLC) and GPC equipped with a multiple-angle laser light scattering detector (GPC−MALLS) to determine molecular weights of eluting molecules. Research goals included the following: (1) the observation of monomeric and oligomeric molecules' dynamics; (2) the integration of resultant PDD dynamics into a comprehensive analysis of the rates of polymerization for molecules observed; (3) the evaluation of reaction rate constants as a function of the reactant's molecular size. Complementary analyses of high molecular weight thermoplastic samples were performed.

Overall Reaction Model. During a major portion of the cure,[1,3] only carboxylic acid propagation sites are observed, indicating a rate-limiting step. Acid/epoxy reactions slowly form alcohols; whereas, the alcohol/anhydride reaction rapidly re-forms acidic propagation sites. Polyether formation is absent when both DGEBA and NMA are present. Although published reaction mechanisms have variants in terms of chemical intermediates, they can be reduced to a simplified, overall reaction sequence.[6,8] In this regard an acid end group (I···AH) on a polymer chain reacts with an epoxy moiety (E) on a monomeric molecule, forming an ester bond and a chain terminal hydroxyl site (I···AEH). The latter spontaneously reacts with the anhydride (A), forming a second ester and re-forming the carboxylic acid (I···AEAH), perpetuating the propagation reaction sequence. Chain links resulting from PGE and NMA are represented by E and A, respectively. The residual from the initiator is I and the propagating chain end is H.

In an abbreviated notation P_j denotes a linear, polymeric species with the chemical structure $IA(EA)_jH$. The degree of polymerization is j. The chain-initiated polymerization has been modeled[6,8] as a series of propagation reactions:

$$P_j + E \xrightarrow{k} P_{j+1} \tag{1}$$

Note that chemical intermediates and associated reactions have been lumped into the rate-limiting step.[1,3,6,8] For batch polymerizations conservation principles yield

$$\frac{d[P_j]}{dt} = k[E]([P_{j-1}] - [P_j])$$

where time is t, the rate constant is k and the PGE's molar concentration is represented as [E]. Sequential integrations, subject to initial conditions $[P_j(0)] = 0$; $j > 0$, yield the Poisson molar distribution:[12,13]

$$[P_j] = [P_0(0)]\frac{\tau^j \exp(-\tau)}{j!} \tag{2}$$

The concentration of propagation sites equals the initial initiator concentration $[P_0(0)]$. Dimensionless time τ is defined by the eigenzeit transform $d\tau = k[E]\,dt$.

Moments are absolutely convergent; therefore, limits are unique:

$$\sum_{j=0}^{\infty}[P_j] = [P_0(0)] \tag{3}$$

$$\sum_{j=0}^{\infty} j[P_j] = [P_0(0)]\tau \tag{4}$$

$$\sum_{j=0}^{\infty} j^2[P_j] = [P_0(0)](\tau^2 + \tau) \tag{5}$$

Equation 3 indicates an invariant, cumulative number of propagation sites (one per polymeric molecule), whereas eq 4 reveals that the mass of the resin at a given conversion is proportional to the extent of reaction expressed through τ.

The set of parallel, propagation reactions shown as eq 1predict an exponential decay for the monomer:

$$[E] = [E(t^*)]\exp(-[P_0(0)](t - t^*)) \tag{6}$$

The time to initially achieve an isothermal state during the cure is t^* and the monomer concentration at that time is $[E(t^*)]$. From the definition of the conversion, conservation principles plus eq 4, conversion ρ may be shown to be proportional to τ:

$$\rho = \frac{[E(0)] - [E(\tau)]}{[E(0)]} = \frac{[P_0(0)]}{[E(0)]}\tau \tag{7}$$

Experimental Section

Resin Preparation. The raw materieals used and their purity and suppliers were as follows: (1) 1,2-epoxy-3-phenoxypropane (phenyl glycidyl ether or PGE, 98.9%/chromatography, 150.17 Da, Aldrich Chemical Co.), (2) methyl-5-norbornene-2,3-dicarboxylic anhydride (nadic methyl anhydride or NMA, 89.5%/titration or 93.4%/chromatography, 178.19 Da, Aldrich Chemical Co.), and (3) *N*,*N*-dimethylbenzylamine (BDMA, 99.0% min, 0.2% max moisture, 135.21 Da, Aldrich Chemical Co.). Chromatograms for each revealed a single peak. PGE/NMA/BDMA were mixed at the molar ratio of 1:1:0.05. One formulation was prepared by adding 25.02815 g of PGE to a tarred beaker. To this was added 29.69703 g of NMA followed by 1.12657 g of BDMA. The initiator *n*-propanol (IH) was then added before mixing the contents of the beaker. A PGE/NMA/BDMA/IH formulation was partitioned into several 5 mL vials which were placed in a preheated, electric oven with forced air circulation. Temperature was controlled to within ±0.5 °C of the set point. At preset times vials were removed and quenched in an ice bath. Sample solutions were made with a concentration of 0.005 g resin/ml solvent (acetonitrile) and stored at −10 °C. Although care was exercised to prepare resins with stoichiometric ratios, this is not a requirement for the chain-growth polymerization. If excess anhydride were formulated, at complete conversion of the oxiranes, the excess would simply remain. If an excess of oxiranes are formulated, conversion will stop prior to 100%. The addition of monomers at the propagating chain end will have but a small effect on the resin's average molecular weight. This is very distinct from that which is experienced by a step-growth polymerization.

HPLC. Waters' chromatographic pumps, UV detector, and μBondapak C_{18}−CN column (with guard column) constituted the HPLC system. A gradient separation method was used with water and acetonitrile (both HPLC grade, Aldrich). The polarity of the mobile phase was adjusted linearly over a period of 1 h, starting from 40 vol % acetonitrile and ending with pure acetonitrile. The overall flow rate was kept constant at 1 mL/min. The UV detector was set at a sensitivity of 0.02 and at a wavelength of 280 nm. The sample volume injected equaled 100 μL.

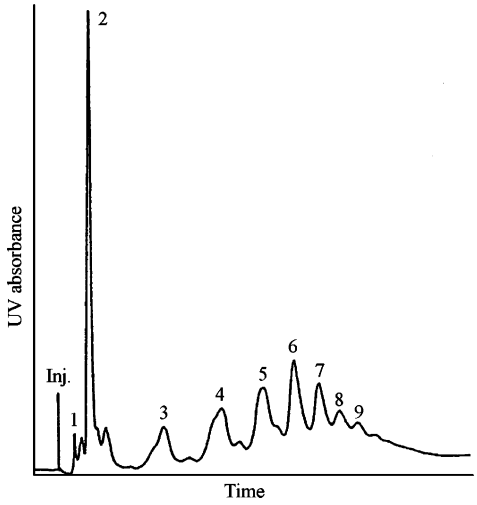

Figure 1. Representative HPLC chromatogram for the PGE/NMA/BDMA cure (initiator/anhydride ratio 0.15, 80 °C, 240 min): (1) NMA; (2) PGE; (3) P_1; (4) P_2; (5) P_3; (6) P_4; (7) P_5; (8) P_6; (9) P_7.

GPC—MALLS. The GPC system consisted of three Waters' Styragel 7.8 × 300 mm columns (HR0.5, HR1.0 and HR2.0) and one chromatographic pump (Waters 590) with HPLC grade toluene (Aldrich) as the mobile phase at a flow rate of 0.75 mL/min. A miniDAWN laser light scattering photometer (Wyatt Technology) was connected at the end of the GPC columns. A Millipore in-line 0.2 μm filter was placed between the pump and the injector. A Waters 410 differential refractometer, placed after the miniDAWN, was used as the concentration detector. detectors were computer interfaced with ASTRA software. Samples were prepared by dissolving 0.1 g resin in 5 mL of toluene. The injection volume was 100 μL.

Oligomeric Reaction Kinetics

The polymerization of PGE/NMA/BDMA/IH mixtures with initial molar composition 1:1:0.05:0.15 was investigated. Figure 1 is a representative gradient separation for a reaction mixture cured at 80 °C for 4 h. Monomers and about 10 oligomers were resolved. Areas and locations of elution bands were observed as a function of oxirane conversion. Linear chain configurations yield molecules that elute in the order of increasing j as indicated. HPLC chromatograms also provided indirect information associated with chemical intermediates present. Intermediates of nearly the same molecular weight have different interactions with the mobile phase and stationary phase, causing unequal retention times. The band assignment emphasizes degree of polymerization and parallels assignments by Dark et al.[14] and Shiono et al.[15] and was consistent with examinations of molecular weight distributions measured by GPC−MALLS analyses.

The area of each elution band represents the mass contribution of all chemical groups comprising the molecules. When UV is the concentration detector, the extinction coefficients for the anhydride and catalyst are insignificant compared to that for PGE (see Figure 1) because of the conjugation effect on absorbance by the benzyl ring:

$$\text{area}_j \cong j[\text{P}_j] \tag{8}$$

Since PGE becomes distributed between the monomer and the resin's chain links

$$[\text{E}(t)] + \sum_{j=1} j[\text{P}_j] = [\text{E}(0)]$$

Therefore, terms appearing in the first moment may be evaluated from

$$j[\text{P}_j] = \frac{\text{area}_j}{\text{area}_{\text{PGE}} + \sum_{j=1} \text{area}_j}[\text{E}(0)] \tag{9}$$

Subject to the degree of polymerization assignment j for a band, the molar concentration of molecules $[P_j]$ can be calculated.

The concentration of the initiator at time zero is the sum of the alcohol added and impurities. Since a considerable amount of alcohol was used in studies addressing oligomers, it is reasonable to approximate the initiator's concentration as the initial concentration of these hydroxyl groups minus the contributions for the fractionated oligomers $[P_o] = [I(0)] - \sum_{j=1}[P_j]$. The conversion of PGE equals the summation of areas corresponding to the oligomers divided by the summation of areas for oligomeric molecules and PGE.

Monomer Dynamics. Figure 2 shows that PGE decayed exponentially for cures at 80 °C, which is consistent with eq 6. A first-order reaction dominated to a conversion of 0.78. The intercept reflects an initial, nonisothermal segment of the cure. A cold sample was placed in the oven and a period of time was required to achieve the cure temperature.

Poisson PDD Analysis. The values of relative mass concentration were determined by the area of each component divided by the total area of all bands in the chromatogram. Equation 9 was used to determine the normalized molar concentration $[p_j]$ ($[p_j] = [P_j]/[E(0)]$) for several oligomers. Results appear in Figure 3. Molecules p_0 decayed rapidly. The dynamics for p_1 and p_2 pass through maxima, whereas the trajectories for p_3 and p_4 tend to increase before approaching an asymptote at a high conversion.

PDD data were fit to the Poisson molar distribution, subject to eqs 2 and 9:

$$\tau = j - 1\sqrt{\frac{\text{area}_j}{\text{area}_1}(j-1)!} \tag{10}$$

Equation 10 was used to evaluate the eigenzeit transform τ from observed PDDs. The average of a set of τ's at the time of sampling permitted calculation of a theoretical PDD. Results are presented in parts a and b of Figure 4 and show appreciable deviation between data and theoretical PDDs, especially at low degrees of polymerization. In addition, eq 6 failed to correlate measured conversion dynamics when these τ's were used.

FTIR analysis of PGE/NMA/BDMA/IH fractions revealed characteristic bands (ester, 1740 and 1175 cm^{-1}; carboxyl, 1600 and near 1420 cm^{-1})[16] indicating that when epoxides and anhydrides are present, the addition of the carboxyl to the epoxide group was markedly preferred. No hydroxyl bands or ether bands were spectrally identified. Such are consistent with constraints used in the derivation of eq 1 and observations reported by Antoon and Koenig.[1] Therefore, the constraint of a rate constant independent of degree of polymerization was examined.

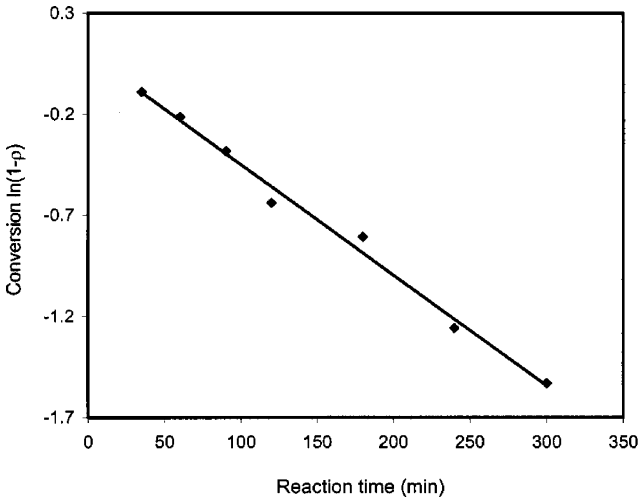

Figure 2. Monomer decay for PGE/NM (80 °C, initiator/anhydride ratio 0.15).

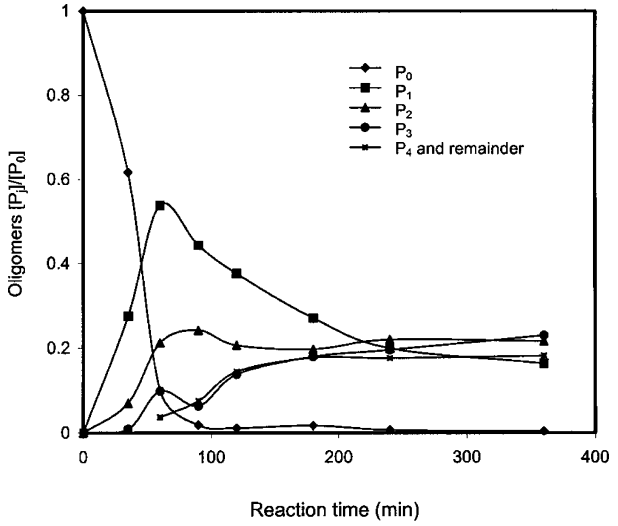

Figure 3. Oligomeric dynamics for PGE/NMA/BDMA (80 °C, initiator/anhydride ratio 0.15).

Gold PDD Analysis. Experimentally measured PDD's as a function of cure allowed for interpreting the overall rate constant as a function of degree of polymerization. For $[P_0]$

$$\frac{d[P_0]}{dt} = -k_0[E][P_0]$$

The derivative $d[P_0]/dt$ was evaluated at several time intervals based on the experimental $[P_0]$ vs t curve in Figure 3. Coupled with experimentally measured monomer concentrations the rate constant k_0 was calculated. For higher molecular weight oligomers,

$$\frac{d[P_j]}{dt} = k_{j-1}[E][P_{j-1}] - k_j[E][P_j]$$

and

$$\sum_0^j \frac{d[P_j]}{dt} = -k_j[E][P_j] \qquad (11)$$

Equation 11 enabled a sequential solution for rate constants k_j listed in Table 1. Analyses were conducted at different conversions. A degree of scatter in k_j was observed. Nonetheless, there is a significant difference between k_0 and the other k_j's, indicating that the reactivity of linear chains decreases by a factor of approximately three once the first epoxide/anhydride linkage has been added. The decrease in the propagation rate constant may be the result of factors such as steric shielding by the pendent benzene ring on the oxirane chain link and/or electron density gradients again imbued by the presence of the aromatic group.

Table 1. Propagation Rate Constant k_j

j	least-squared $k_j \times 1000$ (mol·L^{-1}·min^{-1})	$k_j \times 1000$ range (mol·L^{-1}·min^{-1})
0	15.68	14.57−16.28
1	4.72	4.51−4.79
2	4.59	4.32−4.91
3	4.24	4.11−4.35
4	4.37	4.31−4.47
5	4.68	4.39−4.88
6	4.81	4.77−4.91
7	4.09	N/A

The overall polymerization consists of propagation reactions with rate constant k_p with a distinct initiation reaction having a rate constant k_0:

$$P_0 + E \xrightarrow{k_0} P_1 \quad \text{(initiation)}$$

$$P_j + E \xrightarrow{k_p} P_{j+1} \quad j \geq 1 \text{ (propagation)}$$

By introducing the ratio α

$$\alpha = k_0/k_p$$

and dimensionless time τ

$$d\tau = k_p[E]\,dt$$

sequential integrations with the aid of an integration factor $\exp(\tau)$ yield

$$[P_j] = \frac{\alpha[P_0(0)]}{1-\alpha}\left[\frac{\exp(-\alpha\tau)}{(1-\alpha)^{j-1}} - \sum_{i=0}^{j-1}\frac{\tau^i \exp(-\tau)}{(1-\alpha)^{j-i-1}i!}\right] \qquad (12)$$

Conversion becomes

$$\rho = \frac{[P_0(0)]}{[E(0)]}\left[\tau + \left(\frac{\alpha-1}{\alpha}\right)(1-\exp(-\alpha\tau)\right] \qquad (13)$$

Gold[17] derived eqs 12 and 13.

A numerical fit of experimental PDD's using eq 12 was conducted. The previous differential analysis yields an initial estimate of the value for the ratio of rate constants α. The integral analysis mainly resulted in adjustments to the parameter τ, although some fine-tuning of α was needed. Results proved satisfactory, as can be seen from curves appearing in Figure 4, parts a and b. Note that τ's obtained using the Gold distribution are smaller than those based on the Poisson distribution. A satisfactory fit of conversion data was now achieved using eq 13.

GPC—MALLS Results. PGE/NMA/BDMA oligomeric reaction mixtures were also analyzed by GPC−MALLS to examine molecular mass assignments. Values for the refractive index increment were provided by Podzimek and Kašánek.[18] Figure 5 compares the mass distribution curves for a reaction mixture at 240 min obtained by both analyses. For comparison, results of

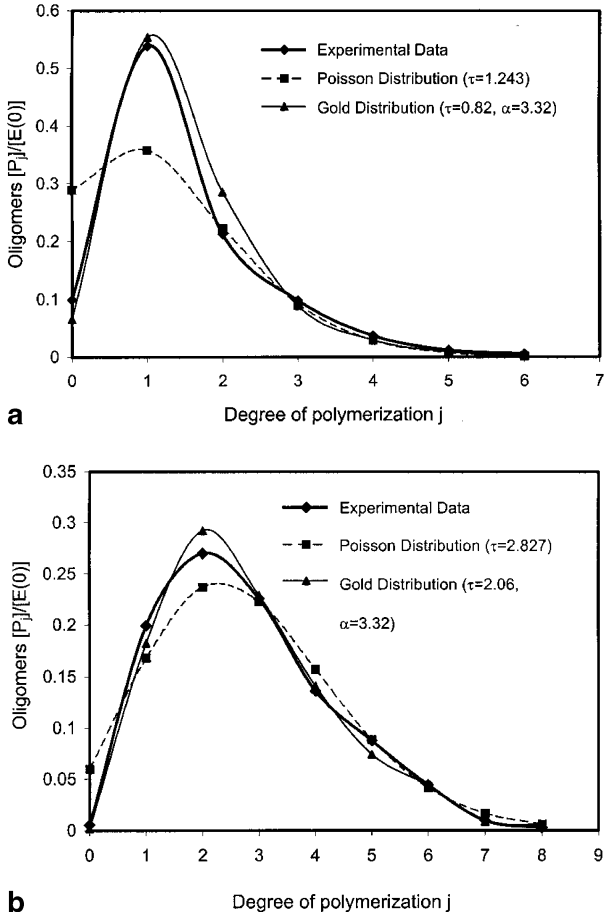

Figure 4. Theoretical-experimental comparison of PDDs: (a) PGE/NMA/BDMA (60 min at 80 °C, initiator/anhydride ratio 0.15); (b) PGE/NMA/BDMA (180 min at 80 °C, initiator/anhydride ratio 0.15).

HPLC analysis was converted to a cumulative weight distribution as a function of molar mass using relationships for the molar mass of molecules P_j:

$$MW_j = jMW_E + (j+1)MW_A + MW_I \qquad (14)$$

and weight fractions

$$\frac{W_j}{W} = \frac{\text{area}_j}{\sum_{j=1}\text{area}_j} = \frac{MW_j[P_j]}{\sum_{j=1}MW_j[P_j]} \qquad (15)$$

The weight of molecules with a degree of polymerization j is W_j and the cumulative weight of oligomeric and polymeric molecules is W. Data graphed in Figure 5 indicate excellent agreement between the two methods.

Polymeric Analysis

High molecular weight epoxy/anhydride resins were prepared by curing a PGE/NMA/BDMA/IH mixture with the initial molar composition 1:1:0.05:0.01 at 90 °C. Polymeric reaction kinetics were studied by observing the molecular weight distribution as a function of cure using the GPC−MALLS method.

Monomer Decay Dynamics. Figure 6 illustrates GPC chromatograms for the reaction mixture collected at times noted in minutes. As time increased the monomer fraction diminished and the polymer fraction increased and shifted to higher molecular weights.

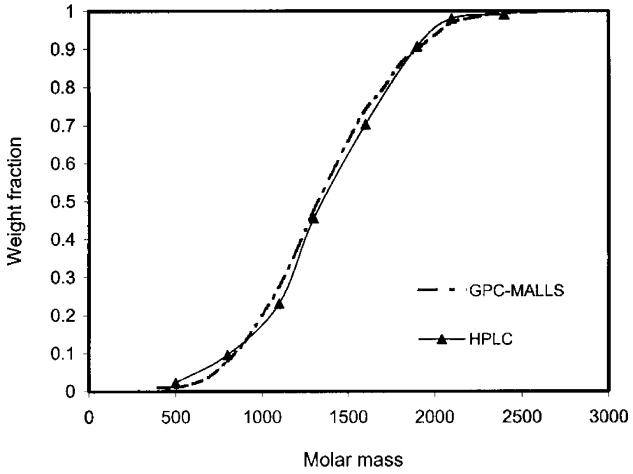

Figure 5. Comparison of cumulative weight fractions by HPLC and GPC−MALLS (PGE/NMA/BDMA 240 min, 80 °C, initiator/anhydride ratio 0.15).

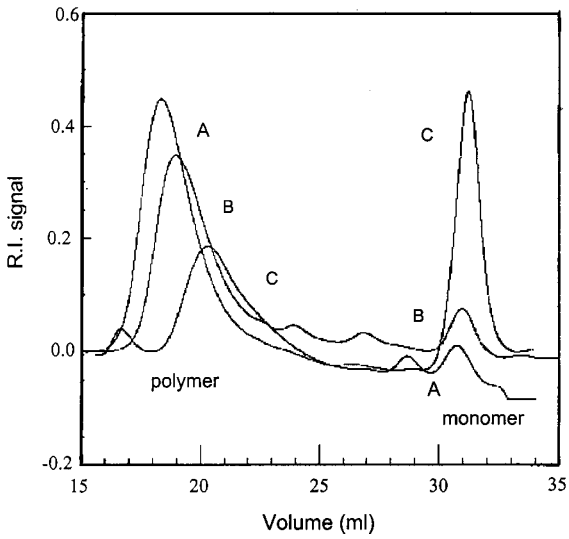

Figure 6. Chromatograms of PGE/NMA/BDMA reaction mixture (90 °C, initiator/anhydride ratio 0.01): (A) 240 min; (B) 160 min; (C) 60 min.

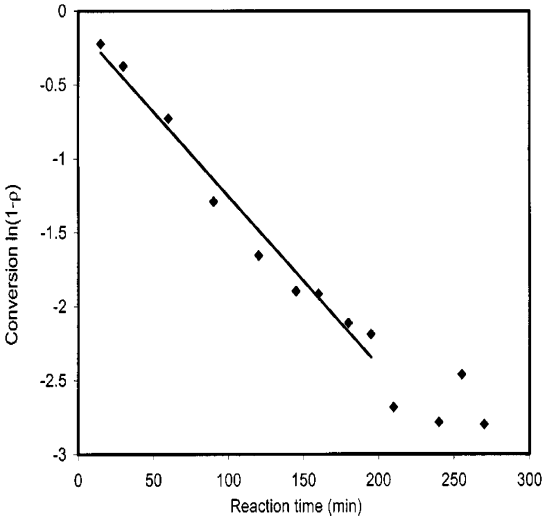

Figure 7. Monomer decay for PGE/NMA/BDMA at 90 °C (initiator/anhydride ratio 0.01).

Conversion was calculated from the areas of polymeric and monomeric peaks at each sampling time. Figure 7 presents the resultant monomer decay. First-order

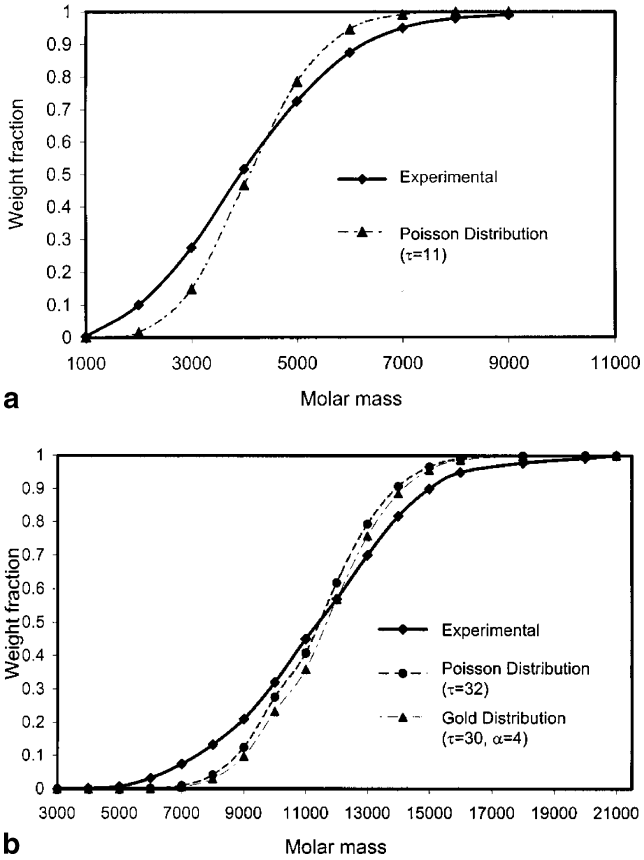

Figure 8. Molecular weight distribution of (a) PGE/NMA/BDMA (60 min, 90 °C, initiator/anhydride ratio 0.01) and (b) PGE/NMA/BDMA.

kinetics fit the curve up to a conversion of 0.80. A slowing of the reaction rate occurred at times greater than 150 min. The cure is a typical example of vitrification where overall diffusion control can become operative at high conversions. The glass transition temperature T_g for the resin eventually approaches or exceeds the reaction temperature T. While well above T_g, the dependence of the rate constant on temperature is governed by an Arrhenius expression; in the glass transition region its dependence on T is determined by segmental chain mobility. Near T_g, the rate constant can be approximated by free-volume theory: [19,20,21]

$$\ln k \propto \frac{T - T_g}{T - T_g + c^g}$$

The above equation indicates that k should approach zero when $T_g - T = c^g$. The constant c^g is about 50 K. Experimental results show that the practical limit for the curing process corresponding to $T_g - T$ is equal to 25−35 K.[19,20] At high extents of reaction, rate constants have been expressed by[22]

$$k(\rho) = \frac{k_0}{1 + \exp[C(\rho - \rho_d)]} \tag{16}$$

The initial reaction rate constant is k_0, the strength parameter is C, conversion is ρ, and the constant ρ_d determines when the change occurs. The form of the function allows the rate constant to be relatively constant for $\rho < \rho_d$ and to decrease rapidly after ρ_d. Data were subjected to a least-squares fit and yielded

Table 2. Changes in Polydispersity for PGE/NMA Polymerization (90°C, Initiator/Anhydride Ratio 0.01)

reaction time (min)	polydispersity M_w/M_n exptl	Poisson parameter t	polydispersity M_w/M_n calcd
60	1.502	11	1.08
90	1.362	18.5	1.05
120	1.179	21.7	1.043
180	1.138	25	1.038
240	1.102	32	1.03

Table 3. Cumulative Molar Concentration for PGE/NMA/BDMA (90°C, Initiator/Anhydride Ratio 0.01)

reaction time (min)	$\sum [P_j]/[E(0)]$
30	0.0423
60	0.0406
90	0.0376
120	0.0348
180	0.0315
240	0.0307
300	0.0291

the values $C = 25.06$, $\rho_d = 0.852$ and k_0=0.0982 mol·L^{-1}·min^{-1}.

PDD Analysis. Information was also gained from measurements of molecular distributions associated with polymeric molecules. Since the Gold and Poisson distributions converge at high degrees of polymerization, the Poisson distribution was used as a basis. Subject to large degrees of polymerization, eqs 2 and 4 yield the differential weight distribution as a function of j and τ:

$$\frac{W_j}{W} = \frac{\tau^{j-1} e^{-\tau}}{(j-1)!} \tag{17}$$

A trial-and-error method was used to find a value for τ such that the molecular weight-average of the theoretical Poisson mass distribution equaled the molecular weight-average for the sample. Representative curves are shown in Figure 8, parts a and b. Subject to equal average molecular weights, experimental distributions are slightly broader than Poisson distributions. As conversion increased deviations decreased. This trend may be observed from the polydispersity index (the ratio of the weight-average molecular weight to the number-average molecular weight) listed in Table 2. The Gold distribution[17] also failed to improve the data fit, as can be seen in Figure 8b. The Poisson and Gold distributions have been shifted to emphasize their similarities at this average molecular weight.

The normalized cumulative molar concentration of molecules was also evaluated using eqs 2, 4, and 7:

$$[P_j] = \frac{[E(0)] - [E(t)]}{j} \frac{W_j}{W} = \frac{\rho[E(0)]}{j} \frac{W_j}{W}$$

and

$$\frac{\sum_{j=1}^{\infty}[P_j]}{[E(0)]} = \frac{\rho}{W}\sum_{j=1}\left(\frac{W_j}{j}\right) \tag{18}$$

The result assumes that the decay rate for the initiator P_0 is sufficient to drive its concentration to zero. This constraint is consistent with Figures 4a,b and 8a,b. In Table 3 results of calculations based on eq 18 are tabulated. Two observations are noteworthy: (1) The experimental cumulative molar concentrations were

consistently greater than the normalized initiator concentration $p_0(0) = 0.01$. (2) The cumulative molar concentration of molecules diminished with increasing conversion. The former correlate with impurities in the monomers that act as co-initiators. However, the decreasing population of molecules is interesting in light of the breadth of the weight fraction distributions. A minor, competing reaction may exist that broadens the latter slightly and at the same time diminishes the number of molecules, such as a competing termination by combination reaction, ie. an esterification reaction may be present. However, this idea was not developed. There is a good fit between theory and experimental data.

Discussion

A major emphasis exists in the area of predicting a thermosetting resin's properties from molecular chain topology.[13] Elastically active chain junctions or branch nodes are predicted to contribute to the equilibrium rubber modulus. Chemical reactions ultimately control their molar dynamics. Thus, accurate reaction models are needed in endeavors to fully comprehend the significance of formulation and conversion on these significant variables. Research[23] is focused on the commercial epoxy based on DGEBA/NMA/BDMA. Since DGEBA and PGE have nearly identical chemical structures, the latter serves as a model compound to the former in the area of developing realistic, overall reaction models. Predictions are examined through analyses of the sol fraction.

Results of this study clearly show that a greatly simplified, overall, chain-initiated model is capable of analyzing observed molecular distributions in the thermoplastic resin formulation, both when the resin's average molecular weight is very low and when it is high. Subject to FTIR analysis, the initiator is believed to rapidly react with the anhydride, converting an alcohol site into an acid group. Resultant molecules then experience a slow, rate-determining step that results in the insertion of an epoxy, which again is rapidly followed by the addition of an anhydride.[1,6,16] Our examination of oligomeric dynamics suggests that the rate constant for initiation, the first addition of the epoxy, is distinct from the rate constant for similar reactions with higher molecular weight oligomers. Such is consistent with results reported on reactions with low molecular weight compounds. The molecule's chemical structure in the neighborhood of the reacting end group can affect its chemical reactivity. The Gold distribution, which incorporates distinct initiation and propagation rate constants, yielded simulations that accurately fit data when compared with the one rate constant Poisson distribution. Molar distributions of resins with number-average molecular weights near 5000 and 13 000 were adequately approximated by either distribution since simulations converged. Evidence does exist that minor, competing reactions are present that slightly broaden the distribution and result in a diminished cumulative number of molecules in the resin.

References and Notes

(1) Antoon, M. K.; Koenig, J. L. *J. Polym. Sci.* **1981**, *19*, 549.
(2) Trappe, V.; Burchard, W.; Steinmann, B. *Macromolecules* **1991**, *24*, 4738.
(3) Matějka, L.; Lovy, J.; Pokorný, S.; Bonchal, K.; Dušek, K. *J. Polym. Sci., Polym. Chem. Ed.* **1983**, *21*, 2873.
(4) Luston, J.; Manasek, Z.; Kulickova, M. *J. Macromol. Sci., Chem. A* **1978**, *12*, 995.
(5) Tanaka, Y.; Kakiuchi, H. *J. Appl. Polym. Sci.* **1963**, *7*, 1063.
(6) Tadros, R.; Timm, D. C. *Macromolecules* **1995**, *28*, 7441.
(7) Garton, A.; Daly, J. H.; Stevenson, W. T. K. *J. Polym. Sci., Polym. Chem. Ed.* **1986**, *24*, 2383.
(8) Nielsen, J. A.; Chen, S. J.; Timm, D. C. *Macromolecules* **1993**, *26*, 1369.
(9) Woo, E. M.; Seferis, J. C. *J. Appl. Polym. Sci.*, **1990**, *40*, 1237.
(10) Park, S.-J.; Kwak, G.-H.; Sumita, M.; Lee, J.-R *Polym. Eng. Sci.* **2000**, *40*, 2569.
(11) Samios, D.; Castiglia, S.; Pesce da Silveira, N.; Stassen, H. *J. Polym. Sci. B: Polym. Phys.* **1995**, *33*, 1857.
(12) Flory, P. J. *J. Am. Chem. Soc.* **1940**, *62*, 1561.
(13) Dotson, N. A.; Galvan, R.; Laurence, R. L.; Tirrell, M. *Polymer Process Modeling*; VCH Publishers: Cambridge, U.K., 1996.
(14) Dark, W. A.; Conard, E. C.; Crossman, L. W., Jr. *J. Chromatogr.* **1974**, *91*, 247.
(15) Shiono, E.; Karino, I.; Ishimura, A.; Eneomoto, J. *J. Chromatogr.* **1980**, *193*, 243.
(16) Chian, W. Ph.D. Dissertation, University of Nebraska-Lincoln, **2002**.
(17) Gold, L. *J. Chem. Phys.* **1958**, *28*, 91.
(18) Podzimek, Š.; Kašánek, A. *J. Appl. Polym. Sci.* **1999**, *74*, 2432.
(19) Rozenberg, B. A. *Adv. Polym. Sci.* **1986**, *78*, 113.
(20) Luňák, S.; Vladyka, K.; Dušek, K. *Polymer* **1978**, *19*, 931.
(21) Sperling, L. H. *Introduction to Physical Polymer Science*, 2nd ed.; John Wiley & Sons: New York, 1992.
(22) Cole, K. C. *Macromolecules* **1991**, *24*, 3093.
(23) Chian, W.; Timm, D. C. *Macromolecules* **2004**, *21*, 8098.

MA049293X